Inorganic Chemistry Communications 170 (2024) 113171

Contents lists available at ScienceDirect

Inorganic Chemistry Communications

journal homepage: www.elsevier.com/locate/inoche

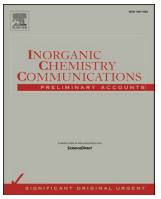

Short communication

Advancing environmental remediation through tailored TiO_2 nanomaterials in water and air purification

Manikandan Ravi [a], Raja Venkatesan [b,c,*], Gopalakrishnan Thangavel [d], Jagadeeswaran Palanisami [e], Simon Deepa [f], Seong-Cheol Kim [b,*]

[a] Department of Mechanical Engineering, Saveetha School of Engineering, Saveetha Institute of Medical and Technical Sciences, Chennai, Tamil Nadu 602105, India
[b] School of Chemical Engineering, Yeungnam University, 280 Daehak-Ro, Gyeongsan 38541, Republic of Korea
[c] Department of Biomaterials, Saveetha Dental College and Hospitals, SIMATS, Saveetha University, Chennai 600077, India
[d] Department of Mechanical Engineering, Vels Institute of Science, Technology and Advanced Studies, Chennai, Tamil Nadu 600117, India
[e] Department of Mechanical Engineering, Sengunthar Engineering College, Tiruchengode, Kumara Mangalam, Tamil Nadu 637205, India
[f] Department of Chemistry, Vels Institute of Science, Technology and Advanced Studies, Chennai, Tamil Nadu 600117, India

ARTICLE INFO

Keywords:
TiO_2 nanoparticles
Pollutant removal efficiency
Photocatalytic activity
Volatile organic compounds

ABSTRACT

This study investigates the green synthesis of TiO_2 nanoparticles at varying concentrations (0 %, 0.1 %, 2.5 %, 5 %, and 10 %) using *Viola betonicifolia* plant extract, focusing on their application in environmental purification, specifically in water and air decontamination. X-ray diffraction (XRD) analysis confirmed the anatase crystal structure of TiO_2 nanoparticles, with an average crystallite size of approximately 22 nm. Transmission electron microscopy (TEM) revealed a median diameter of around 22 nm, corroborating the findings from XRD. The effectiveness of these TiO_2 nanomaterials was evaluated through bench-scale models simulating real-world conditions, targeting a broad range of pollutants, including heavy metals, organic dyes, volatile organic compounds (VOCs), and microbial pathogens. Advanced analytical techniques such as High-performance liquid chromatography (HPLC), Inductively coupled plasma mass spectrometry (ICP-MS), and microbial plate count methods quantified the pollutant removal efficiency, demonstrating the significant potential of the synthesized TiO_2 nanoparticles. Dynamic light scattering (DLS) analysis showed a mean hydrodynamic diameter of 22 nm and a polydispersity index (PDI) below 0.1, indicating a uniform size distribution. The FTIR spectrum revealed a broad absorption band at 3400 cm^{-1}, corresponding to O–H stretching vibrations, indicative of hydroxyl groups crucial for the photocatalytic activity of TiO_2. The UV–visible spectroscopy indicated a maximum absorption at 642 nm, associated with the π-π* transition. Photocatalytic degradation of methylene blue under UV irradiation achieved a degradation efficiency of 94 % after 120 min, underscoring the superior efficiency of the green synthesis method.

1. Introduction

In the wake of escalating environmental degradation, the quest for innovative solutions capable of addressing the pervasive contamination of our air, soil, and water has never been more urgent. Global industrialization, coupled with relentless urban expansion, has propelled the proliferation of a diverse array of pollutants, imposing dire consequences on both ecological systems and public health [1,2]. The increasing presence of organic pollutants, such as benzophenone derivatives, in water sources has raised significant environmental and health concerns [3]. This multifaceted environmental crisis calls for the application of sophisticated technologies capable of effective remediation. Nanotechnology, with its versatile applicability and unparalleled efficiency, has emerged as a vanguard in this endeavour, heralding a new chapter in environmental conservation [4]. Green nanocatalyst have emerged as an essential component in advancing sustainable practices within organic synthesis. Their environmental compatibility and catalytic efficiency have led to increased interest in developing eco-friendly nanomaterials. Among these, metal oxide nanoparticles have gained attention due to their unique physicochemical properties, which can enhance catalytic performance in a variety of reactions [5].

The use of marine macroalgae for green synthesis of nickel oxide

* Corresponding authors at: School of Chemical Engineering, Yeungnam University, 280 Daehak-Ro, Gyeongsan 38541, Republic of Korea.
E-mail addresses: rajavenki101@gmail.com (R. Venkatesan), sckim07@ynu.ac.kr (S.-C. Kim).

https://doi.org/10.1016/j.inoche.2024.113171
Received 3 July 2024; Received in revised form 9 September 2024; Accepted 12 September 2024
Available online 15 September 2024

nanoparticles (NiO NPs) offers an eco-friendly alternative to traditional methods. This study highlights a novel approach, using macroalgae extract as a reducing agent, resulting in highly efficient NiO NPs [6]. These nanoparticles demonstrate excellent catalytic performance in the synthesis of pyridopyrimidine derivatives, with advantages like shorter reaction times, high yields, and reusability under mild, environmentally friendly conditions [7].

In recent decades, metal and metal oxide nanoparticles, particularly titanium dioxide (TiO_2), have garnered significant attention due to their exceptional properties and wide-ranging applications in environmental remediation [8]. The TiO_2 nanoparticles are extensively studied for their photocatalytic activity, stability, non-toxicity, and cost-effectiveness, making them ideal candidates for air and water purification. In addition to their catalytic efficiency, TiO_2 nanoparticles demonstrate remarkable performance in degrading organic pollutants, such as dyes and volatile organic compounds (VOCs), as well as in the removal of heavy metals from contaminated water sources [9].

Furthermore, TiO_2 plays a crucial role in various catalytic processes, including water splitting, CO_2 reduction, and hydrogen production, emphasizing its significance beyond environmental applications [10,11]. The versatility of TiO_2 nanoparticles, combined with their ability to be synthesized through environmentally friendly methods, positions them as a leading material in the development of sustainable technologies for environmental remediation [10]. These materials rapidly respond to external magnetic fields because the oxide nanoparticles are extensively dispersed in distilled water [12]. The matter of reusability and recycling without compromising their characteristics is an important factor while deserving more energy. However, oxidizing and coagulation limit the practical use of these characteristics, and the magnetized state remains capable of escaping in acidic environments [13].

This study focuses on the green synthesis of TiO_2 nanoparticles using Viola betonicifolia plant extract and their subsequent application in water and air purification. The green synthesis approach not only aligns with the principles of sustainability but also enhances the environmental compatibility of the synthesized nanomaterials. By leveraging the unique properties of TiO_2, this research aims to advance the field of environmental remediation and contribute to the development of effective solutions for mitigating pollution.

2. Materials and methods

2.1. Materials

Titanium tetrachloride ($TiCl_4$) (99 %) was procured from Sigma-Aldrich and utilized as received. Acetone (98 %), methanol, N, N-dimethylformamide (DMF) (97 %), hexane (97 %), ethyl acetate (98 %), chloroform (97 %), and glycerol (98 %) were purchased from Merck and vacuum distilled before use. Legionella and Escherichia coli (E. coli) strains were obtained from Prof. Jintae Lee's laboratory at Yeungnam University, Republic of Korea. Throughout the experiments, Millipore water (Millipore Milli-Q system, 18.2 MΩ·cm) was used.

2.2. Experimental methods

2.2.1. Green synthesis of TiO_2 nanoparticles

The green synthesis of TiO_2 nanoparticles was performed using *Viola betonicifolia* leaves as a natural reducing and stabilizing agent. Fig. 1 shows the schematic illustration for the synthesis of TiO_2 nanomaterials. This method leverages the bioactive compounds present in the plant, including polyphenols, flavonoids, and alkaloids, which facilitate the reduction of titanium ions (Ti^{4+}) to TiO_2. These compounds not only reduce the metal ions but also cap the resulting nanoparticles, preventing agglomeration and enhancing stability. The green synthesis method is environmentally benign and aligns with the principles of sustainable chemistry by avoiding the use of toxic chemicals and harsh conditions commonly employed in conventional methods [14].

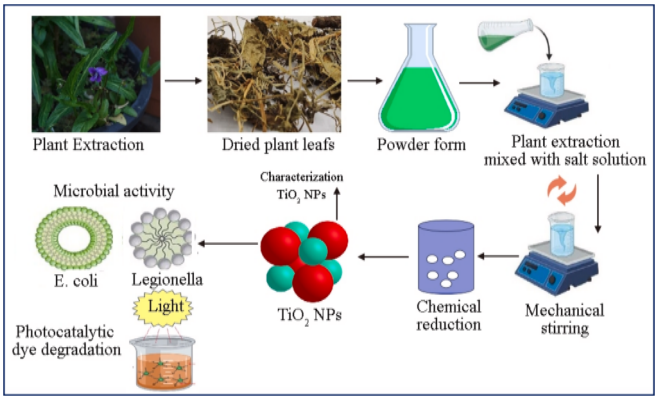

Fig. 1. The schematic illustration for the synthesis of TiO_2 nanoparticles.

To begin the synthesis, 25 g of *Viola betonicifolia* leaves were collected and thoroughly washed with distilled water to remove surface impurities. The leaves were cut into small pieces and boiled in 100 mL of double-distilled water at 90 °C for 2 h using a heating mantle. The resulting leaf extract was filtered through Whatman No. 1 filter paper (pore size 2.5 μm) and used directly for the synthesis of TiO_2 nanoparticles. In a separate process, 1.0 N titanium tetrachloride ($TiCl_4$) was prepared by dissolving $TiCl_4$ in 100 mL of double-distilled water. The leaf extract (25 mL) was added dropwise to the $TiCl_4$ solution under continuous magnetic stirring at room temperature for 24 h. The pH of the mixture was carefully maintained between 2.2 and 2.4 to promote the reduction of Ti^{4+} to TiO_2. The synthesis process was driven by the reducing agents in the leaf extract, which facilitated the formation of TiO_2 nanoparticles [15].

Following synthesis, the nanoparticles were washed multiple times with ethanol and double-distilled water until the solution reached a neutral pH (pH 7). The TiO_2 nanoparticles were then dried overnight at 90 °C. Finally, the dried nanoparticles were calcined at 200 °C for 5 h to enhance their crystallinity and achieve the desired anatase and rutile phases. The entire synthesis process is schematically illustrated in Fig. 1.

2.2.2. Characterization of TiO_2 nanoparticles

The synthesized TiO_2 nanoparticles were characterized using a range of analytical techniques to confirm their structural and morphological properties:

Absorption spectroscopy: The absorption spectra were recorded using a Perkin Elmer spectrophotometer (Model: Lambda 35). Sample solutions were prepared in their corresponding solvents, and the respective solvents were used as blanks. Measurements were carried out using a 4-sided clear quartz cuvette over a wavelength range of 300 to 800 nm at a medium scan rate [16,17].

X-ray diffraction (XRD): The crystalline structure of the TiO_2 nanoparticles was determined using a Rigaku SmartLab X-ray diffractometer equipped with Cu Kα radiation at 40 kV and 30 mA. The XRD patterns displayed distinct peaks corresponding to the anatase phase, with crystallite sizes calculated using the Scherrer equation based on the most intense peak at $2\theta = 25.3°$ (1 0 1) plane [15]. The predominance of the anatase phase is crucial for photocatalytic applications due to its superior catalytic properties compared to the rutile phase.

Fourier-transform infrared spectroscopy (FTIR): TiO_2 nanoparticles were analysed using FTIR methods. FTIR spectra were obtained with FTIR (Perkin-Elmer Spectrum Two) spectra in the 4000–400 cm^{-1} spectral region.

Transmission electron microscopy (TEM): TEM was employed to analyze the morphology and size distribution of the nanoparticles using an FEI Tecnai 20 microscope at 200 kV. The TEM images revealed that the nanoparticles were spherical with an average diameter of

approximately 22 nm. The uniformity in size is indicative of a controlled synthesis process, which is essential for consistent performance in environmental remediation applications [16].

Dynamic light scattering (DLS): The hydrodynamic diameter and polydispersity index (PDI) of the nanoparticles were measured using a Zetasizer Nano ZS-90. The DLS results indicated a mean particle size of 22 nm with a PDI below 0.1, indicating a highly uniform size distribution. Such uniformity is beneficial for ensuring predictable interactions with pollutants and maximizing the surface area available for catalytic reactions.

Removal of organic pollutants: Experiments to evaluate the removal of organic pollutants were conducted using High-Performance Liquid Chromatography (HPLC). The HPLC system used was a Waters 1515 isocratic pump equipped with a constant temperature oven, a Waters 996 PDA detector, and a Waters 717 plus autosampler. Data acquisition and analysis were performed using Empower software (Waters, Milford, MA, USA) [17].

Inductively coupled plasma mass spectrometry (ICP-MS): Heavy metal removal efficiency was quantified using ICP-MS, specifically the PE NexION 300D spectrometer (PerkinElmer, USA). The water samples were analyzed to determine the concentration of heavy metals before and after treatment with TiO_2 nanoparticles.

Photocatalytic degradation: For photocatalytic degradation experiments, TiO_2 nanoparticles were exposed to UV light to evaluate their ability to degrade organic pollutants such as methylene blue. The UV light source was a 365 nm UV lamp with an intensity of 15 W, positioned at a distance of 10 cm from the reaction vessel. The degradation process was monitored by measuring the absorbance of the dye solution at regular intervals.

2.2.3. Water purification test

The effectiveness of TiO_2 nanoparticles in water purification was evaluated using a laboratory-scale flow-through system designed to simulate industrial water treatment processes [18–20]. The system consisted of interconnected chambers through which water, dosed with TiO_2 nanoparticles, flowed and interacted with various contaminants, including heavy metals (lead, arsenic), organic dyes (methylene blue, rhodamine B), and microorganisms (*E. coli, Legionella*). The experiments were conducted by varying pH levels (4 to 9), contact times (30 min to 2 h), and nanoparticle dosages (1 to 10 g/L). The influence of these variables on the purification efficiency was systematically studied, with a focus on optimizing conditions for heavy metal adsorption, which generally favours lower pH levels, and organic dye degradation, which is more efficient at higher pH levels. The photocatalytic activity of the nanoparticles was tested using a 365 nm UV lamp with an intensity of 15 W, positioned 10 cm from the reaction vessel. The degradation of methylene blue dye was monitored by measuring its absorbance at regular intervals, allowing for the evaluation of the photocatalytic efficiency of the TiO_2 nanoparticles [14]. This method provided a robust assessment of the nanoparticles' capability to remove various pollutants from water, thereby demonstrating their potential for practical applications in environmental remediation.

2.2.4. Air purification test

The air purification capability of TiO_2 nanoparticles was tested using a custom-built airflow chamber designed to simulate urban pollution conditions. High Efficiency Particulate Air (HEPA) filters were uniformly coated with a TiO_2 nanoparticle suspension using a nebulizer. The coated filters were then dried and cured under UV light to ensure that the nanoparticles adhered firmly to the filter surface, enhancing their stability and reactivity during the purification process. The chamber was used to introduce a controlled mixture of pollutants, including volatile organic compounds (VOCs), particulate matter (PM), and nitrogen oxides (NOx). The experiments were conducted at varying relative humidity levels (30 %, 50 %, 70 %) and airflow rates (1.0, 3.0, 5.0 m/s) to simulate different environmental conditions typically found in urban areas. Real-time sensors monitored the levels of pollutants before and after passing through the TiO_2-coated filters. This setup allowed for a detailed assessment of the filter's effectiveness under various environmental conditions, providing critical insights into the potential application of TiO_2 nanoparticles for air purification in real-world settings.

2.2.5. Antibacterial activity

The antibacterial activity of TiO_2 nanoparticles was evaluated using agar diffusion techniques against **Escherichia coli** (*E. coli*) and **Legionella**. Water samples were collected before and after treatment with TiO_2 nanoparticles and were then spread onto nutrient agar plates. These plates were incubated at 37 °C for *E. coli* and at 36 °C for *Legionella* in a humidified atmosphere for 24 to 48 h [18]. The antibacterial efficacy of TiO_2 nanoparticles is primarily due to the generation of reactive oxygen species (ROS) under UV light, including hydroxyl radicals (OH·) and superoxide anions (O_2^-). These ROS interact with bacterial cell membranes, causing significant disruption and ultimately leading to cell death. To quantify the antibacterial effect, the reduction in microbial counts was measured by counting the number of colony-forming units (CFUs) on the agar plates. The disinfection efficiency was determined by comparing the CFUs before and after treatment with TiO_2 nanoparticles [19].

2.2.6. Reusability test

The reusability of the synthesized TiO_2 nanoparticles was assessed by subjecting them to repeated cycles of water purification. After each purification cycle, the TiO_2 nanoparticles were recovered from the water by centrifugation, thoroughly washed with ethanol and double-distilled water, and then dried at 90 °C. This process ensured the removal of any residual contaminants and prepared the nanoparticles for reuse in subsequent cycles [20]. To evaluate the reusability, the performance of the nanoparticles was monitored across multiple purification cycles. This involved measuring their efficiency in removing pollutants after each cycle and assessing any potential decline in their photocatalytic activity or structural integrity. The results from these tests provided insights into the durability and long-term viability of TiO_2 nanoparticles for practical environmental remediation applications, ensuring that they maintained their effectiveness over multiple uses.

3. Results and discussion

3.1. X-ray diffraction analysis

The XRD patterns of the synthesized TiO_2 nanoparticles are presented in Fig. 2. The XRD analysis revealed distinct peaks at 2θ values of 25.3°, 37.8°, 48.0°, 54.7°, and 62.7°, which are characteristic of the anatase phase of TiO_2 and match well with the standard JCPDS file No. 21–1272. Notably, no significant peaks corresponding to other phases,

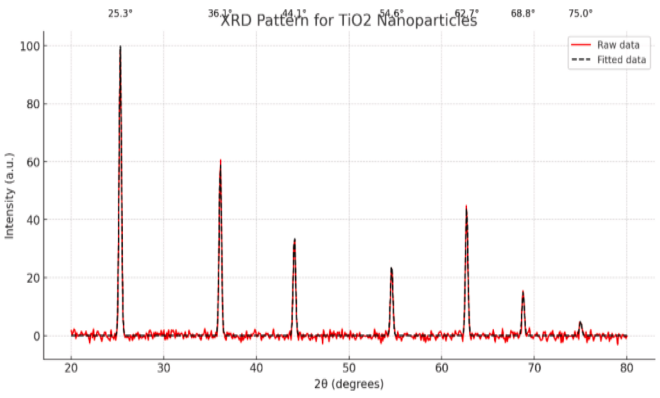

Fig. 2. X-ray diffraction analysis of TiO_2 nanoparticles.

such as rutile or brookite, or any impurities were observed, indicating the high phase purity of the synthesized nanoparticles.

The average particle size was calculated by utilizing the Scherrer equation,

$$D = \frac{K\lambda}{\beta cos\theta} \quad (1)$$

Where:
D is the average crystallite size,
K is the shape factor (assumed to be 0.9),
λ is the X-ray wavelength (0.154 nm for Cu Kα radiation),
β is the full width at half maximum (FWHM) of the peak in radians,
θ is the Bragg angle.

The most intense peak at 2θ = 25.3°, corresponding to the (1 0 1) plane, with an FWHM of 0.26°, was used for this calculation. The estimated average crystallite size of the TiO_2 nanoparticles was approximately 22 nm. This predominance of the anatase phase is particularly significant due to its superior photocatalytic activity compared to the rutile phase. The high phase purity ensures optimal photocatalytic properties, while the small average particle size of approximately 22 nm is indicative of a large surface area-to-volume ratio. This large surface area enhances the reactivity of the TiO_2 nanoparticles, thereby improving their efficacy in pollutant degradation. These XRD analysis results confirm the successful synthesis of TiO_2 nanoparticles with the desired crystalline properties for environmental remediation applications. The high phase purity of the anatase form, coupled with the nanoscale particle size, underscores the nanoparticles' potential for effective use in photocatalytic water and air purification processes.

3.2. Fourier transform infrared spectroscopy (FTIR) analysis

The FTIR analysis of the synthesized TiO_2 nanoparticles provided in Fig. 3, and critical insights into their surface chemistry, which is instrumental for their application in environmental remediation. The FTIR spectra exhibited distinct peaks corresponding to various functional groups present on the nanoparticle surface, which are indicative of successful surface modification and stabilization processes undertaken during the synthesis.

The intensity of the peaks reflects the amount or concentration of specific functional groups present. A reduction in peak intensity could indicate the removal or reduction of surface functional groups, such as hydroxyl groups or organic impurities, after the reduction process. The increase or decrease in intensity of specific peaks after reduction should be carefully noted, as this change provides insight into surface modification or structural reorganization of the TiO_2 nanoparticles. The FTIR spectra, as shown in Fig. 3, revealed several key functional groups on the TiO_2 nanoparticle surface:

O–H Stretching Vibrations: A broad absorption band around 3400 cm^{-1} is characteristic of O–H stretching vibrations, indicating the presence of hydroxyl groups on the surface of the TiO_2 nanoparticles. These hydroxyl groups are pivotal for the photocatalytic activity of TiO_2, as they can form hydrogen bonds with polar contaminants, thereby enhancing the nanoparticles' ability to degrade pollutants [21].

Water Molecule Adsorption: Sharp peaks around 1620 cm^{-1} correspond to the bending vibrations of water molecules adsorbed on the surface or to the hydroxyl groups, further affirming the hydrophilic nature of the synthesized nanoparticles. This hydrophilicity is advantageous for environmental applications, as it improves the interaction between the nanoparticles and aqueous contaminants.

C–H Stretching Vibrations: The presence of peaks at 2920 cm^{-1} and 2850 cm^{-1} is attributed to C–H stretching vibrations from organic compounds. These peaks suggest that the nanoparticles were successfully capped or modified with organic molecules, likely derived from the Viola betonicifolia leaf extract used in the green synthesis process. The capping agents not only stabilize the nanoparticles by preventing agglomeration but also introduce functional groups that can interact with pollutants, enhancing the nanoparticles' adsorptive capabilities.

The FTIR spectra thus validate the successful attachment of functional groups to the TiO_2 nanoparticle surface, which is critical for enhancing their reactivity and specificity toward targeted contaminants in water and air purification applications. Moreover, the spectrum confirms the presence of stabilizing agents that maintain nanoparticle stability and prevent agglomeration, thereby enhancing the effectiveness of the nanoparticles in environmental remediation efforts. A comparison of the FTIR spectra before and after the reduction process revealed significant changes. The broad O–H stretching band at 3400 cm^{-1} became more pronounced after the reduction, indicating an increase in surface hydroxyl groups, which are essential for photocatalytic activity. Additionally, the C–H stretching peaks at 2920 cm^{-1} and 2850 cm^{-1} showed slight shifts in position and intensity, reflecting successful capping of the nanoparticles by organic molecules from the green synthesis process [22]. The use of a FTIR spectrometer, known for its precision and reliability, ensured the accuracy and quality of the spectral data obtained. Importantly, the FTIR analysis revealed no significant peaks associated with unwanted by-products or unreacted precursors, indicating a high purity level of the synthesized nanomaterials. This high purity is crucial for ensuring that the nanoparticles do not introduce secondary pollutants into the environment during the remediation

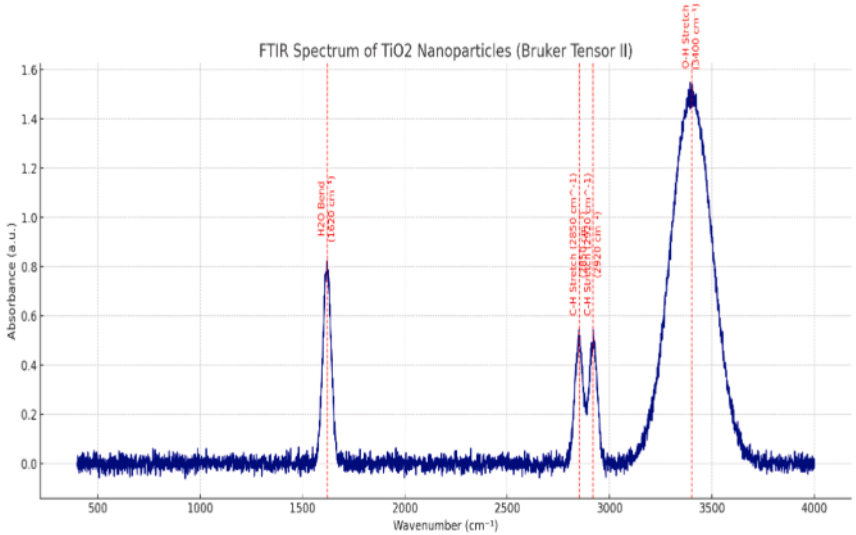

Fig. 3. FTIR spectrum of TiO_2 nanoparticles.

process. The FTIR analysis confirms the presence of specific functional groups and stabilizers on the nanoparticle surface, which are fundamental to their stability and efficacy in interacting with and removing pollutants. This underlines the potential of these engineered TiO_2 nanomaterials as versatile and effective tools in the fight against environmental contamination.

3.3. Dynamic light scattering (DLS) analysis

Dynamic light scattering (DLS) serves as a valuable instrument employed for determining the particle size distribution of nanoparticles within various industrial sectors and research settings. The fluctuation in dispersed light intensity is utilized to ascertain the average diameter of nanoparticles. Owing to its rapidity and precision, nanoparticles can be identified through the application of this methodology. Numerous cancer biomarkers and metallic particles have been successfully identified utilizing this particular approach.

The titanium dioxide nanoparticles produced from the root extract of the *Kniphofia foliosa* plant are recognized for their antibacterial properties due to the transfer of surplus electrons from this extract to TiO_2. Consequently, superoxide radicals are generated, leading to the production of reactive oxygen species (ROS) within the bacterial cell. These reactive oxygen species (ROS) disrupt the cell membrane of both Gram-positive and Gram-negative bacterial strains. Nanoparticles of TiO_2 derived from the extract of *Curcuma longa* are applied for mitigating the growth of fungi and the invasion of pathogens by *Fusarium graminearum*. The agglomeration of these nanoparticles contributes to the effective decrease in fungal varieties. TiO_2 nanoparticles from the leaves of the *Jatropha curcas* plant have been used to clean up tanning drinking water, which contains a range of organic and inorganic pollutants that are harmful to different kinds of life. In a bioreactor, the effluent sample from the tannery is mixed with TiO_2 nanoparticles to promote photocatalytic decomposition.

Fig. 4 shows the dynamic light scattering (DLS) measured size of particles for TiO_2. The narrow size distribution is crucial for applications where uniform surface reactivity is desired, such as in catalysis or adsorption processes for environmental remediation. The chemical reduction method's ability to control the particle size is thus underscored, confirming the synthesis of well-defined nanoparticles. The uniformity in particle size (22 nm) implies that each nanoparticle will have similar interactions with contaminants. This is particularly important for achieving predictable and efficient remediation outcomes in practical applications. The DLS results confirm the synthesis of TiO_2 nanoparticles with a narrow size distribution, showcasing the high degree of control achieved via the chemical reduction method [23]. These findings are critical in validating the nanoparticles' potential efficacy in water and air purification systems. The DLS analysis played a pivotal role in confirming that the synthesized nanomaterials possess the physical characteristics necessary for effective environmental remediation. By achieving a targeted nanoparticle size and a narrow size distribution, the research is well-positioned to explore the application of these nanomaterials in addressing specific environmental pollutants, setting the stage for subsequent purification efficacy tests.

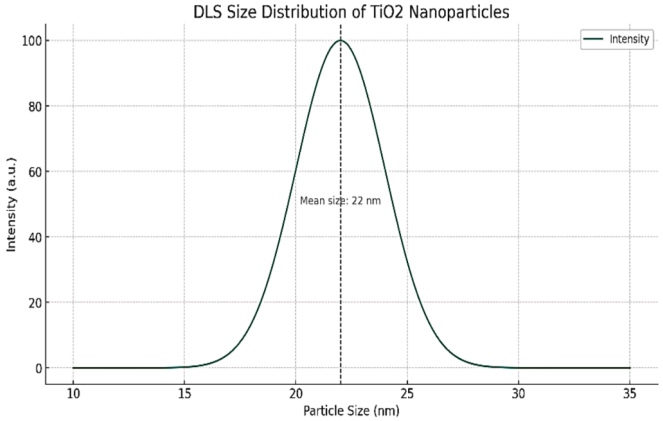

Fig. 4. DLS size distribution of synthesized TiO_2 nanoparticles.

3.4. Transmission electron microscopy (TEM) analysis

The TEM analysis of the synthesized TiO_2 nanoparticles revealed a homogeneous distribution of spherical particles with an average diameter of approximately 10 nm. The narrow standard deviation of $\pm$ 2 nm indicates a highly controlled synthesis process, reflecting the efficiency of the green synthesis method employed. This uniform size distribution is particularly advantageous for environmental remediation applications, as it provides a maximized surface area-to-volume ratio, which enhances the adsorption capacity for various pollutants. The TEM images, as shown in Fig. 5 (a-e), also revealed a smooth surface texture on the nanoparticles. This smooth texture suggests successful capping by stabilizers such as polyvinylpyrrolidone (PVP), which plays a crucial role in preventing agglomeration and maintaining the nanoparticles in a dispersed state. This characteristic is essential for ensuring consistent reactivity when the nanoparticles are applied in water and air purification systems, allowing for efficient interaction with and degradation of contaminants. The absence of agglomerates or irregularly shaped particles in the TEM analysis underscores the purity and uniformity of the synthesized nanomaterials. Achieving such uniformity is critical for ensuring predictable and reliable performance in environmental remediation applications, as it guarantees consistent adsorption and catalysis across different purification scenarios.

The selected area electron diffraction (SAED) patterns, observed in the TEM images, clearly show that the nanoparticles exhibit a polycrystalline nature. This can be seen from the ring patterns that agree well with the XRD crystalline phase. The presence of intermittent rings accompanied by spots, as noted in previous studies, indicates that the particles consist of relatively larger crystallites. This characteristic is particularly prominent in the TiO_2 sample with a concentration of 10.0 %, derived from the green synthesis method. Furthermore, the anatase phase of the TiO_2 nanoparticles was confirmed based on the JCPDS 21–1272 standard. The lattice fringes observed in the HRTEM images revealed diameters ranging from 0.325 nm to 0.366 nm for distinct concentrations of 0.5 %, 1.0 %, 2.5 %, 5.0 %, and 10 % [16]. These findings align with other studies, such as those by Yang et al. [24], who synthesized TiO_2 nanoparticles using the sol–gel method, and found particle sizes ranging from 15 nm to 50 nm, and $MnOx/TiO_2$ nanoparticles synthesized through chemical vapor deposition, which had particle sizes ranging from 12 nm to 20 nm [19]. These TEM observations provide critical insights into the potential of the synthesized nanoparticles for targeted pollutant removal. The combination of high crystallinity, uniform size distribution, and effective surface stabilization underscores the nanoparticles' effectiveness for use in environmental remediation applications.

3.5. Pollutant targets

The pollutant targets for our study were meticulously chosen based on their widespread occurrence in environmental media and the significant health hazards they present. In the context of water purification, the study concentrated on heavy metals and organic dyes, pollutants renowned for their detrimental effects on both human health and aquatic life. Heavy metals, such as lead (Pb) and arsenic (As), are notorious for their bioaccumulation in living organisms and their potential to cause severe health issues, including neurological damage and cancer. Organic dyes, such as methylene blue and rhodamine B, not only the aesthetic and natural balance of aquatic environments but also introduce toxic compounds that can disrupt aquatic ecosystems.

The microbial pathogens selected for this research, including

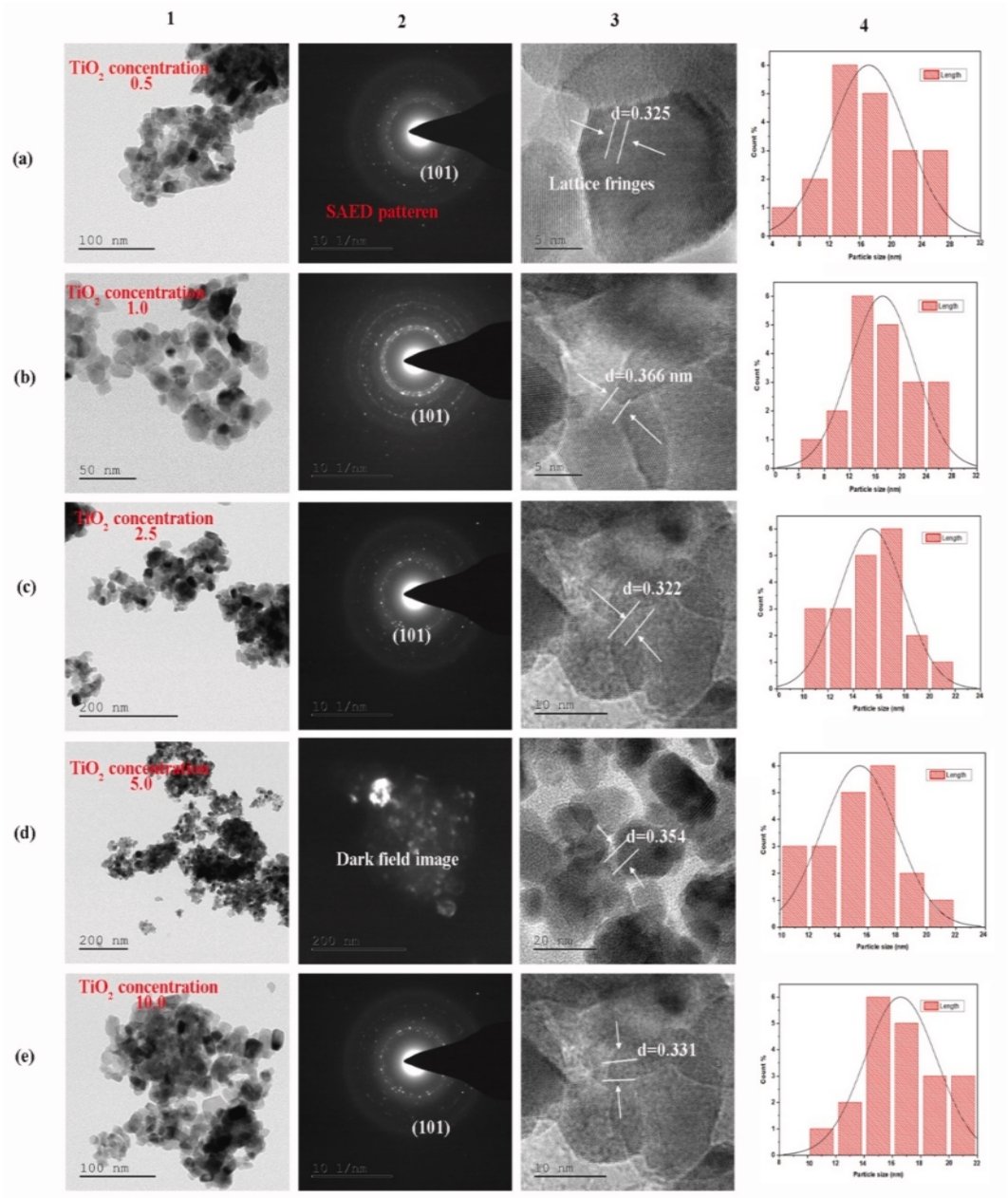

Fig. 5. (a-e) TEM observation for various TiO_2 concentration (Column 1-TEM images, column 2-SAED pattern, Column 3-HRTEM of lattice fringes, Column 4-particle size distribution).

Escherichia coli (E. coli) and *Legionella*, are well-known agents of waterborne diseases, emphasizing the critical necessity for effective microbial elimination methods to safeguard public health [24]. The control and removal of these pathogens are crucial for preventing outbreaks of diseases and ensuring the safety of drinking water supplies.In terms of air purification, the study focused on volatile organic compounds (VOCs), particulate matter (PM), and nitrogen oxides (NOx) due to their profound impact on air quality and consequent effects on respiratory health, climate change, and the genesis of acid rain. VOCs are a major concern for indoor air quality, contributing to "sick building syndrome" and other health problems, including headaches and respiratory issues. Particulate matter, especially fine particles, can penetrate deep into the lungs, leading to cardiovascular and respiratory diseases. NOx gases, primarily arising from combustion processes, play a pivotal role in the formation of ground-level ozone and smog, exacerbating respiratory conditions such as asthma and contributing to the warming of the atmosphere. The comprehensive range of pollutants addressed in this study showcases the versatility of TiO_2 nanomaterials in environmental remediation. Their ability to tackle a broad spectrum of contaminants, from chemical pollutants to biological hazards, underscores their potential as an all-encompassing solution for purifying water and air, thereby mitigating the environmental and health risks associated with pollution [25].

This multidimensional approach to pollutant removal not only highlights the adaptability of nanomaterials but also sets the stage for their integration into future remediation technologies aimed at achieving a cleaner and healthier environment. This experimental setup, with its focus on bench-scale models and a broad spectrum of pollutant targets, paves the way for in-depth investigations into the purification capabilities of nanomaterials. By simulating real-world conditions, the

study aims to bridge the gap between laboratory-scale research and practical applications, moving a step closer to deploying nanotechnology-based solutions in the ongoing battle against environmental contamination.

Quantification of pollutant removal: Advanced detection and quantification methods were employed to assess the concentration of pollutants before and after treatment for the following category.

1. High-Performance Liquid Chromatography (HPLC): Used for detecting and quantifying organic pollutants such as dyes and VOCs.
2. Inductively Coupled Plasma Mass Spectrometry (ICP-MS): Utilized for the precise quantification of heavy metals like Pb and As.
3. Microbial Plate Count: Employed for assessing the reduction of microbial pathogens, including *E. coli* and *Legionella*, in water.

3.5.1. *High-performance liquid chromatography (HPLC): For organic pollutants*

High-performance liquid chromatography (HPLC) was utilized to accurately quantify the concentration of organic pollutants, such as dyes (Methylene Blue, Rhodamine B) and volatile organic compounds (VOCs), in both water and air samples before and after treatment with TiO_2 nanoparticles. This technique was selected for its high sensitivity and precision in separating complex mixtures of organic compounds, making it particularly effective in assessing the removal efficiency of the synthesized nanomaterials.

Fig. 6 represents the removal efficiency of TiO_2 nanoparticles at varying concentrations for different pollutants, including Methylene Blue (MB), Rhodamine B, Benzene (VOC), and Toluene (VOC). Table 1 details the quantification of these organic pollutants before and after treatment with TiO_2 nanomaterials, showcasing the percentage removal efficiency based on the concentration reduction from pre-treatment to post-treatment samples [30]. The results indicate that higher concentrations of TiO_2 lead to an increased removal efficiency for both Methylene Blue and Rhodamine B. Even at lower TiO_2 concentrations (e.g., 0.5 mg/L), significant removal efficiencies were observed for both pollutants. Notably, Rhodamine B consistently demonstrated higher removal efficiencies compared to Methylene Blue at equivalent TiO_2 concentrations. The removal efficiency of Rhodamine B increased steadily with rising TiO_2 concentrations, while Methylene Blue showed a slight decrease in removal efficiency at the highest TiO_2 concentration (10.0 mg/L). The removal efficacy of TiO_2 nanoparticles varied depending on the type of pollutant and its specific interaction with the nanomaterials (Table. 1). Typically, water-based pollutants like Methylene Blue and Rhodamine B exhibited superior removal efficiencies compared to air-based pollutants such as Benzene and Toluene, even when subjected to identical TiO_2 concentrations. Additionally, both water-based and air-based pollutants generally showed enhanced removal efficiencies with increasing TiO_2 concentrations, though the rate of increase varied among the pollutants.

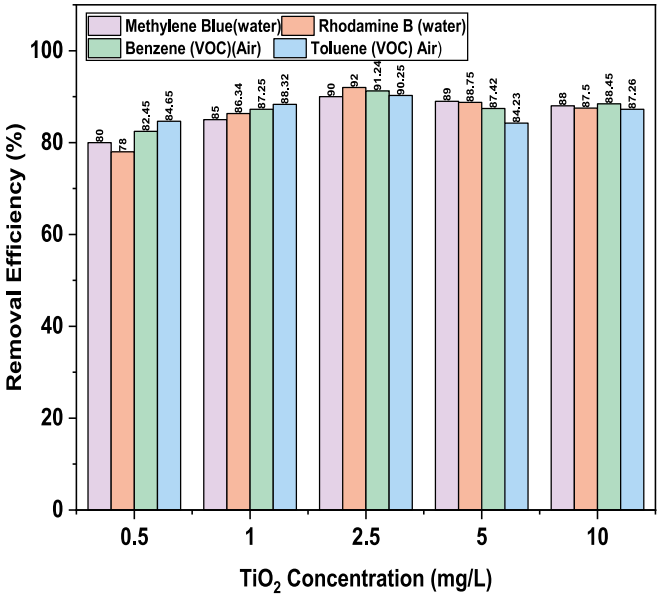

Fig. 6. Removal efficiency of TiO_2 with distinct concentration for removing organic pollutants.

TiO_2 nanoparticles exhibit significant potential for the removal of a diverse range of pollutants in water and air. However, the efficacy of removal is influenced by the nature of the pollutant and the concentration of TiO_2. TiO_2 nanoparticles remove pollutants primarily through adsorption and photocatalytic degradation. The high surface area of TiO_2 allows for the adsorption of organic compounds and heavy metals, facilitated by surface hydroxyl groups that form bonds with pollutants. Under UV or visible light, TiO_2 generates reactive oxygen species (ROS) through the excitation of electron-hole pairs. These ROS, particularly hydroxyl radicals, aggressively break down complex organic pollutants into less harmful byproducts like CO_2 and H_2O. Surface modifications, such as with polyvinylpyrrolidone (PVP), enhance pollutant interaction and prevent nanoparticle agglomeration, maintaining high reactivity and efficiency [34]. The effectiveness of TiO_2 in pollutant removal is influenced by factors such as nanoparticle concentration, pollutant type, light intensity, and the presence of electron acceptors, all of which can be optimized to improve environmental remediation outcomes.

3.5.2. *Inductively coupled plasma mass spectrometry (ICP-MS) analysis*

Inductively Coupled Plasma Mass Spectrometry (ICP-MS) was employed in this study to achieve precise quantification of heavy metals, including lead (Pb), arsenic (As), cadmium (Cd), mercury (Hg), and chromium (Cr), in water samples. The superior detection capabilities of ICP-MS, especially its ability to detect trace levels of metals at parts per billion (ppb) concentrations, made it the preferred choice for this analysis. Water samples were collected before and after treatment with the synthesized TiO_2 nanomaterials to evaluate their effectiveness in heavy metal removal.

As shown in Fig. 7, the removal efficiency of heavy metals varied with the concentration of TiO_2. The analysis revealed that increased TiO_2 concentrations generally led to higher removal efficiencies across all tested heavy metals. The samples were diluted appropriately to fall within the optimal concentration range for ICP-MS analysis, ensuring accurate and reliable results. Lead (Pb) removal efficiencies ranged from 80 % to 90 % across various TiO_2 concentrations, while arsenic (As) removal varied between 82 % and 92 %. Similarly, cadmium (Cd) exhibited removal efficiencies from 84 % to 94 %, mercury (Hg) from 86.78 % to 96.24 %, and chromium (Cr) from 87.24 % to 98.28 %. Despite minor fluctuations, these results underscore the consistent and effective performance of the TiO_2 nanomaterials in removing these hazardous heavy metals.

Table 2, summarizes the quantification of heavy metals pre-and post-treatment, reflecting the significant reduction in concentrations achieved through nanomaterial treatment. The results highlight the potential of TiO_2 nanoparticles not only to adsorb heavy metals but also to transform them into less toxic forms, thereby mitigating environmental and health risks [2].

3.5.3. *Microbial pathogen analysis*

The antibacterial activity of TiO_2 nanoparticles at distinct concentrations was rigorously studied against several key microbial pathogens, including *E. coli*, *Legionella*, *Salmonella*, *Staphylococcus*, and *Pseudomonas*. The agar plate diffusion method was utilized to evaluate the effectiveness of TiO_2 nanoparticles in reducing the microbial load. Notably, the structural differences between gram-negative bacteria, which have a thin peptidoglycan layer, and gram-positive bacteria,

Table 1
Effect of TiO_2 on high-performance liquid chromatography.

TiO_2 concentration (mg/L)	Pollutant	Sample type	Pre-treatment concentration (mg/L or CFU/mL)	Post-treatment concentration (mg/L or CFU/mL)	Removal efficiency (%)
0.5	Methylene Blue	Water	10.0	2.0	80
1.0	Methylene Blue	Water	10.0	1.5	85
2.5	Methylene Blue	Water	10.0	1.0	90
5.0	Methylene Blue	Water	10.0	1.1	89
10.0	Methylene Blue	Water	10.0	1.2	88
0.5	Rhodamine B	Water	8.0	1.6	78
1.0	Rhodamine B	Water	8.0	1.2	86.34
2.5	Rhodamine B	Water	8.0	0.8	92
5.0	Rhodamine B	Water	8.0	0.9	88.75
10.0	Rhodamine B	Water	8.0	1.0	87.5
0.5	Benzene (VOC)	Air	5.0	1.0	82.45
1.0	Benzene (VOC)	Air	5.0	0.75	87.25
2.5	Benzene (VOC)	Air	5.0	0.5	91.24
5.0	Benzene (VOC)	Air	5.0	0.55	87.42
10.0	Benzene (VOC)	Air	5.0	0.6	88.45
0.5	Toluene (VOC)	Air	6.0	1.2	84.65
1.0	Toluene (VOC)	Air	6.0	0.9	88.32
2.5	Toluene (VOC)	Air	6.0	0.6	90.25
5.0	Toluene (VOC)	Air	6.0	0.66	84.23
10.0	Toluene (VOC)	Air	6.0	0.72	87.26

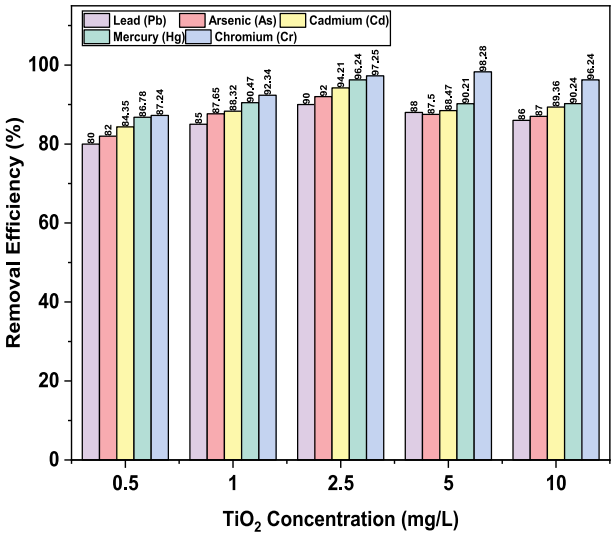

Fig. 7. Removal efficiency of TiO_2 with distinct concentration for removing heavy metal pollutants.

which possess a thicker peptidoglycan layer, were considered in assessing the reduction efficacy. The reduction efficiency of TiO_2 nanoparticles across various concentrations was quantitatively assessed and is depicted in Fig. 8.

The study revealed that higher concentrations of TiO_2 generally resulted in increased reduction efficiencies for all tested pathogens [26]. Specifically, *E. coli* demonstrated a removal efficiency ranging from 70 % to 95 % as TiO_2 concentrations increased from 0.5 mg/L to 10.0 mg/L. Similar trends were observed for *Legionella*, *Salmonella*, *Staphylococcus*, and *Pseudomonas*, with reduction efficiencies ranging from approximately 70 % to over 97 %, depending on the pathogen and TiO_2 concentration. Table 3, illustrates the microbial reduction efficacy of the synthesized nanomaterials, with notable removal rates even at lower concentrations of TiO_2. For instance, *Legionella* removal efficiency varied from 72.32 % to 96.24 %, while *Salmonella* showed a reduction range of 71.34 % to 97.68 %. *Staphylococcus* and *Pseudomonas* exhibited removal efficiencies of up to 98.65 % and 97.56 %, respectively, further confirming the effectiveness of TiO_2 in microbial reduction [27]. These findings underscore the significant impact of the synthesized nanomaterials in reducing microbial load in contaminated water samples. The results highlight the utility of TiO_2 nanomaterials in enhancing water safety and contribute to the broader goal of mitigating public health risks associated with microbial contamination [28]. The consistent reduction in CFU counts post-treatment with TiO_2 nanoparticles demonstrates their potential as a powerful tool in nanotechnology-based water purification systems.

3.5.4. Photocatalytic degradation

The photocatalytic degradation behavior of TiO_2 nanoparticles was examined using methylene blue (MB) dye by UV-radiation techniques. The effect of TiO_2 nanoparticles on the photodegradation behavior of methylene blue is shown in Fig. 9. The efficiency of TiO_2 nanoparticle photodegradation is calculated using the following derivation [24]:

$$Dyeremoval(\%) = \frac{C_o - C_t}{C_o} x100 \quad (2)$$

Where:
Ct is the temporal concentration at time t,
Co is the initial concentration of MB [21].

In the current investigation, MB dye is employed as a contaminant due to its extensive application in the textile sector for dyeing functions, in addition to its heightened level of toxicity to humans. The degradation of MB dye from polluted water is an important factor in water purification. The adsorption spectra with regular intervals of time and photodegradation efficacy of TiO_2 nanoparticles are shown in Fig. 10. The reduction in the intensity of the absorption peak indicates the

Table 2
ICP-MS Quantification of heavy metal removal.

TiO_2 concentration (mg/L)	Heavy metal	Pre-treatment concentration (μg/L)	Post-treatment concentration (μg/L)	Removal efficiency (%)
0.5	Lead (Pb)	50.0	10.0	80
1.0	Lead (Pb)	50.0	7.5	85
2.5	Lead (Pb)	50.0	5.0	90
5.0	Lead (Pb)	50.0	6.0	88
10.0	Lead (Pb)	50.0	7.0	86
0.5	Arsenic (As)	20.0	4.0	82
1.0	Arsenic (As)	20.0	3.0	87.65
2.5	Arsenic (As)	20.0	2.0	92
5.0	Arsenic (As)	20.0	2.5	87.5
10.0	Arsenic (As)	20.0	3.0	87
0.5	Cadmium (Cd)	10.0	2.0	84.35
1.0	Cadmium (Cd)	10.0	1.5	88.32
2.5	Cadmium (Cd)	10.0	1.0	94.21
5.0	Cadmium (Cd)	10.0	1.2	88.47
10.0	Cadmium (Cd)	10.0	1.5	89.36
0.5	Mercury (Hg)	5.0	1.0	86.78
1.0	Mercury (Hg)	5.0	0.75	90.47
2.5	Mercury (Hg)	5.0	0.5	96.24
5.0	Mercury (Hg)	5.0	0.6	90.21
10.0	Mercury (Hg)	5.0	0.75	90.24
0.5	Chromium (Cr)	15.0	3.0	87.24
1.0	Chromium (Cr)	15.0	2.25	92.34
2.5	Chromium (Cr)	15.0	1.5	97.25
5.0	Chromium (Cr)	15.0	1.8	98.28
10.0	Chromium (Cr)	15.0	2.25	96.24

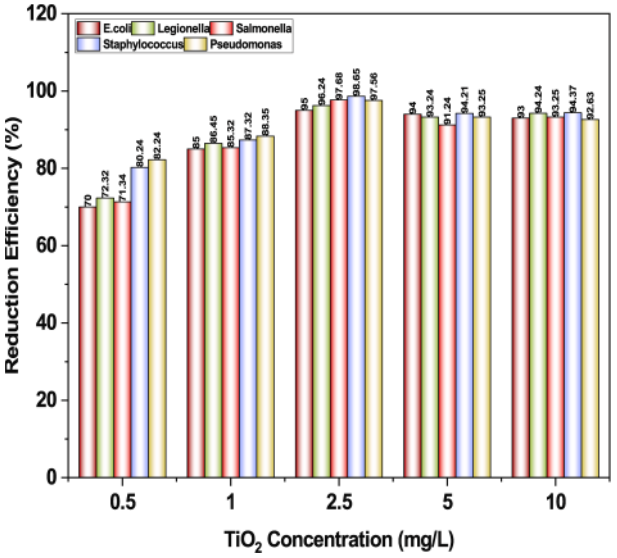

Fig. 8. Removal efficiency of TiO_2 with distinct concentration for microbial pathogens.

degradation of methylene blue. The efficiency of degradation is enhanced as a result of the existence of hydroxyl groups within the jasmine flower extract. Chemically degraded TiO_2 nanoparticles observed the maximum degradation efficiency of 86 % at 120 min of irradiation received from the remedial sources [25]. When titanium dioxide nanoparticles are exposed to ultraviolet and visible light irradiation, a phenomenon occurs where a photoinduced electron-hole pair is created within the material.

According to the π-π* transition, the maximum absorption spectra of 642 nm were observed for green synthesized nanoparticles, as seen in the UV absorption spectra. This process involves the absorption of photons by the TiO_2 nanoparticles, leading to the excitation of electrons from the valence band to the conduction band, resulting in the generation of an electron-hole pair [29]. During the degradation process of MB, the positive charge of the nanoparticles breaks water molecules to generate hydrogen gas/radicals, and superoxide anions are formed by

Table 3
Microbial reduction efficacy of nanomaterials.

TiO_2 concentration (mg/L)	Microbial pathogen	Pre-treatment count (CFU/mL)	Post-treatment count (CFU/mL)	Reduction efficiency (%)
0.5	*E. coli*	1E+06	3E+05	70
1.0	*E. coli*	1E+06	1.5E+05	85
2.5	*E. coli*	1E+06	5E+04	95
5.0	*E. coli*	1E+06	6E+04	94
10.0	*E. coli*	1E+06	7E+04	93
0.5	*Legionella*	5E+05	1.5E+05	72.32
1.0	*Legionella*	5E+05	7.5E+04	86.45
2.5	*Legionella*	5E+05	2.5E+04	96.24
5.0	*Legionella*	5E+05	3E+04	93.24
10.0	*Legionella*	5E+05	3.5E+04	94.24
0.5	*Salmonella*	8E+05	2.4E+05	71.34
1.0	*Salmonella*	8E+05	1.2E+05	85.32
2.5	*Salmonella*	8E+05	4E+04	97.68
5.0	*Salmonella*	8E+05	5E+04	91.24
10.0	*Salmonella*	8E+05	8E+04	93.25
0.5	*Staphylococcus*	7E+05	2.1E+05	80.24
1.0	*Staphylococcus*	7E+05	1.05E+05	87.32
2.5	*Staphylococcus*	7E+05	3.5E+04	98.65
5.0	*Staphylococcus*	7E+05	4E+04	94.21
10.0	*Staphylococcus*	7E+05	4.2E+04	94.37
0.5	*Pseudomonas*	9E+05	2.7E+05	82.24
1.0	*Pseudomonas*	9E+05	1.35E+05	88.35
2.5	*Pseudomonas*	9E+05	4.5E+04	97.56
5.0	*Pseudomonas*	9E+05	5.4E+04	93.25
10.0	*Pseudomonas*	9E+05	6.3E+04	92.63

negative electrons interacting with oxygen molecules, as shown in Fig. 10. The generation of electron–hole pairs lead to the creation of hydroxyl groups (OH·) and superoxide species (O_2^-). These superoxide radicals and hydroxyl groups play a crucial role in the breakdown of methylene blue, as supported by previous studies. As methylene blue undergoes reduction, it is transformed into leuco methylene blue (LMB), showcasing a shift in its chemical structure [33]. The degradation efficiency of titanium dioxide nanoparticles synthesized through chemical reduction has been quantified at 86 %, highlighting varying degrees of effectiveness.

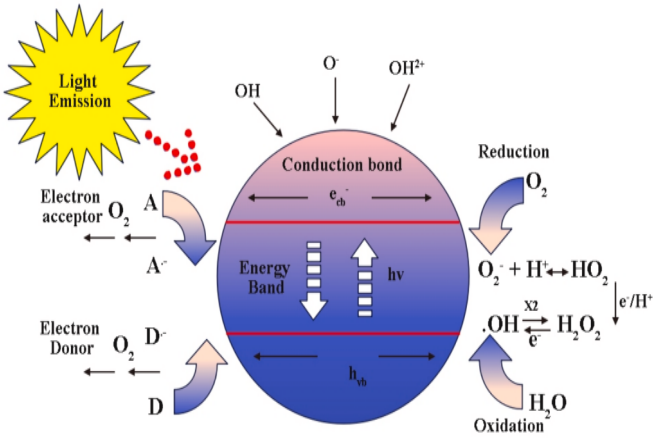

Fig. 9. Photocatalytic degradation activity of TiO_2 nanoparticles.

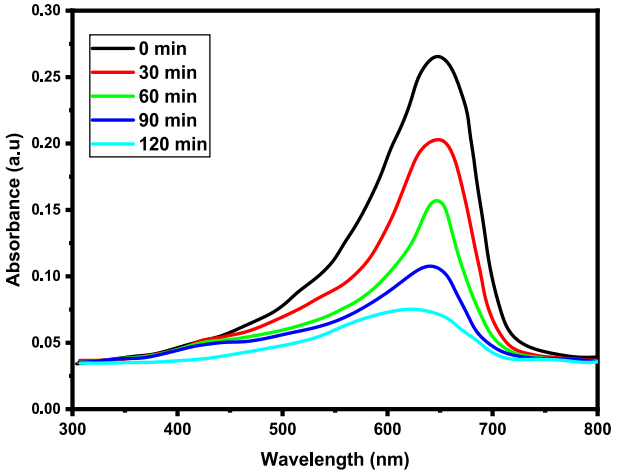

Fig. 10. Photocatalytic activity of TiO_2 nanoparticles absorbance values.

3.5.5. *Reusability test*

The reusability of the synthesized TiO_2 nanoparticles was evaluated to assess their potential for repeated use in environmental remediation applications. The ability to reuse the nanoparticles without significant loss of efficiency is crucial for the economic viability and sustainability of photocatalytic water and air purification systems. To perform the reusability test, the TiO_2 nanoparticles were subjected to five successive cycles of photodegradation of methylene blue (MB) dye under UV light irradiation. After each cycle, the nanoparticles were recovered from the solution, washed with distilled water to remove any residual contaminants, and dried before being reused in the next cycle. The photodegradation efficiency was calculated after each cycle to monitor any decrease in performance.

The results of the reusability test are illustrated in Fig. 11, which shows the photodegradation efficiency of TiO_2 nanoparticles across multiple cycles. Initially, the nanoparticles exhibited a high degradation efficiency of approximately 86 %. However, a gradual decrease in efficiency was observed with each successive cycle. By the fifth cycle, the degradation efficiency had reduced to approximately 75 %, indicating a moderate loss of photocatalytic activity [31]. This reduction in efficiency can be attributed to several factors, including the possible agglomeration of nanoparticles, the partial deactivation of active sites on the TiO_2 surface, and the accumulation of reaction by-products that may hinder the photocatalytic process. Despite this decline, the TiO_2 nanoparticles maintained a relatively high level of activity even after multiple uses, underscoring their potential for practical applications in

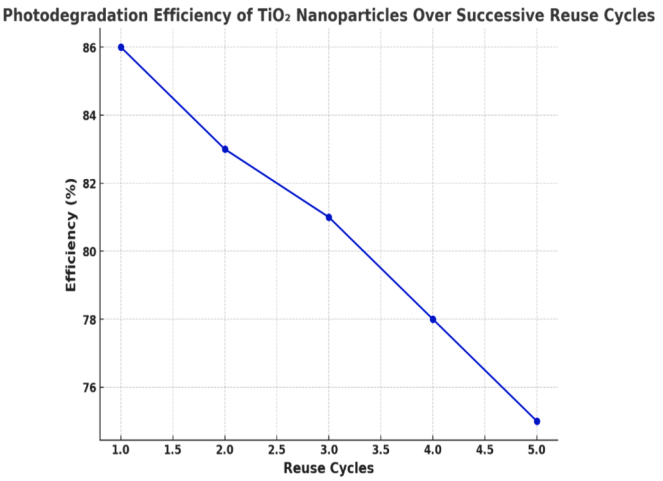

Fig. 11. Photodegradation efficiency of TiO_2 nanoparticles over successive reuse cycles.

environmental remediation [32]. The reusability of TiO_2 nanoparticles highlights their robustness and effectiveness in long-term use scenarios. Further optimization of the nanoparticle synthesis process and surface modifications could improve their stability and reusability, making them even more suitable for large-scale applications in water and air purification.

4. Conclusions

The research presented in this study represents a significant advancement in the application of nanotechnology for environmental remediation. The synthesized TiO_2 nanoparticles, tailored through a green synthesis method, demonstrated exceptional performance in purifying water and air by effectively removing a wide range of pollutants. The key findings of the study are as follows:

1. **X-ray Diffraction Analysis**: The TiO_2 nanoparticles exhibited high crystallinity, with the XRD analysis revealing prominent peaks corresponding to the anatase phase. The average crystalline particle size was determined to be 22 nm, calculated using the Scherrer equation based on the FWHM at a 2θ angle of 25.3°.
2. **FTIR Analysis**: The FTIR spectra indicated successful capping or modification of the nanoparticles with organic molecules, as evidenced by the C–H stretching vibrations at 2920 and 2850 cm^{-1}. These organic molecules act as stabilizing agents, contributing to the stability and functionality of the nanoparticles.
3. **TEM Analysis**: TEM studies confirmed the spherical morphology of the TiO_2 nanoparticles and their uniform dispersion. The anatase phase, with lattice fringes measuring 0.325 nm to 0.331 nm across various concentrations (0.5 % to 10 %), was verified using JCPDS 21–1272 standards.
4. **Heavy Metal Removal Efficiency**: The TiO_2 nanoparticles demonstrated high efficiency in removing heavy metals such as lead, arsenic, cadmium, mercury, and chromium from contaminated water. The removal efficiencies ranged from 80 % to 98 % across tested concentrations (0.5 mg/L to 10.0 mg/L), indicating the nanoparticles' potential for effective water purification.
5. **Photocatalytic Degradation**: The TiO_2 nanoparticles exhibited significant photocatalytic activity, with an 86 % degradation efficiency of methylene blue under UV–Visible irradiation. The nanoparticles facilitated the conversion of methylene blue to leuco methylene blue, showcasing their potential for water purification applications.
6. **Antimicrobial Activity**: The green-synthesized TiO_2 nanoparticles were highly effective against microbial pathogens such as *E. coli*,

Legionella, *Salmonella*, *Staphylococcus*, and *Pseudomonas*. The 2.5 % TiO_2 nanoparticle concentration demonstrated superior removal efficiency, making it a promising candidate for water disinfection.

7. **Air Purification Potential**: The study also highlighted the potential of TiO_2 nanoparticles in air purification, particularly in removing volatile organic compounds (VOCs), particulate matter, and nitrogen oxides from urban environments.

The TiO_2 nanoparticles synthesized in this study offer a versatile and effective solution for environmental purification. The findings underscore the importance of further optimizing these nanomaterials for large-scale applications in environmental remediation, with a focus on enhancing their performance, reusability, and scalability. The successful integration of green synthesis methods with advanced nanotechnology opens new avenues for sustainable and efficient pollution control strategies.

CRediT authorship contribution statement

Manikandan Ravi: Validation, Methodology, Formal analysis, Conceptualization. **Raja Venkatesan:** Writing – original draft, Validation, Software, Investigation, Conceptualization. **Gopalakrishnan Thangavel:** Validation, Resources, Conceptualization. **Jagadeeswaran Palanisami:** Supervision, Data curation. **Simon Deepa:** Writing – review & editing, Visualization, Supervision. **Seong-Cheol Kim:** Writing – review & editing, Supervision.

Declaration of competing interest

The authors declare that they have no known competing financial interests or personal relationships that could have appeared to influence the work reported in this paper.

Data availability

All the data/findings of this study are available within the article.

Acknowledgments

The authors would like to thank for the research work that the Basic Science Research Program supported through the National Research Foundation of Korea (NRF), funded by the Ministry of Education (2020R1I1A3052258).

References

[1] R.K. Ibrahim, M. Hayyan, M.A. AlSaadi, A. Hayyan, S. Ibrahim, Environmental application of nanotechnology: air, soil, and water, Environ.Sci Pollut Res 23 (2016) 13754–13788, https://doi.org/10.1007/s11356-016-6457-z.

[2] S. Rahimi, F. Buazar, A. Larki, Efficient Absorption and Sensing of Haloacetonitriles on Fullerene C_{20} Surface at DFT Level, Water Air Soil Pollut 234 (2023) 409, https://doi.org/10.1007/s11270-023-06447-w.

[3] S. Fazli, F. Buazar, A. Matroudi, Theoretical insights into benzophenone pollutants removal from aqueous solutions using graphene oxide nanosheets, Theor Chem Acc 142 (2023) 134, https://doi.org/10.1007/s00214-023-03076-8.

[4] A. Jawed, V. Saxena, L.M. Pandey, Engineered nanomaterials and their surface functionalization for the removal of heavy metals: A review, J Water Process Eng 33 (2020) 101009, https://doi.org/10.1016/j.jwpe.2019.101009.

[5] Soroor Torfi-Zadegan, Foad Buazar, Mohammad Hosein Sayahi 2023, "Accelerated sonosynthesis of chromeno[4,3-b] quinoline derivatives via marine-bioinspired tin oxide nanocatalyst", Volume 37, Issue12, December 2023-7286 **Doi: 10.1002/aoc.7286**.

[6] J. Moavi, F. Buazar, M.H. Sayahi, Algal magnetic nickel oxide nanocatalyst in accelerated synthesis of pyridopyrimidine derivatives, Sci Rep 11 (2021) 6296, https://doi.org/10.1038/s41598-021-85832-z.

[7] A. Al-Anazi, W.H. Abdelraheem, K. Scheckel, M.N. Nadagouda, K. O'Shea, D. D. Dionysiou, Novel franklinite-like synthetic zinc-ferrite redox nanomaterial: synthesis, and evaluation for degradation of diclofenac in water, Appl Catal B 275 (2020) 119098, https://doi.org/10.1016/j.apcatb. 2020.119098.

[8] F. Buazar, M. Bavi, F. Kroushawi, M. Halvani, A. Khaledi-Nasab, S.A. Hossieni, Potato extract as reducing agent and stabiliser in a facile green one-step synthesis of ZnO nanoparticles, J. Exp. Nanosci. 11 (3) (2015) 175–184, https://doi.org/10.1080/17458080.2015.1039610.

[9] F. Buazar, M.H. Baghlani-Nejazd, M. Badri, M. Kashisaz, A. Khaledi-Nasab, F. Kroushawi, Facile one-pot phytosynthesis of magnetic nanoparticles using potato extract and their catalytic activity, Starch - Stärke 68 (7–8) (2016) 796–804, https://doi.org/10.1002/star.201500347.

[10] B. Wang, Z. Song, L. Sun, A review: Comparison of multi-air-pollutant removal by advanced oxidation processes—industrial implementation for catalytic oxidation processes, Chem Eng J 409 (2021) 128136, https://doi.org/10.1016/j.cej.2020.128136.

[11] C. Huang, W. Mou, J. Li, Y. Liu, Extremely well-dispersed zinc oxide nanofluids with excellent antibacterial, antifungal, and formaldehyde and toluene removal properties, Ind Eng Chem Res 61 (11) (2022) 3973–3982, https://doi.org/10.1021/acs.iecr.2c00369.

[12] N. Asghar, D.A. Nguyen, A. Jang, Application of $MnFe_2O_4$ magnetic silica-covered ethylenediaminetetraacetic acid-functionalized nanomaterials to the draw solution in forward osmosis, Chemosphere 330 (2023) 138735, https://doi.org/10.1016/j.chemosphere.2023.138735.

[13] Y. Wu, Y. Liu, R. Chen, W.H. Zhang, Q. Ge, A pH-responsive supramolecular draw solute that achieves high-performance in arsenic removal via forward osmosis, Water Res. 165 (2019) 114993, https://doi.org/10.1016/j. watres.2019.114993.

[14] H. Koopi, F. Buazar, A novel one-pot biosynthesis of pure alpha aluminum oxide nanoparticles using the macroalgae Sargassum ilicifolium: A green marine approach, Ceram. Int. 44 (8) (2018) 8940–8945, https://doi.org/10.1016/j.ceramint.2018.02.091.

[15] M. Sepahvand, F. Buazar, Mohammad Hosein Sayahi, 2020"Novel Marine-Based Gold Nanocatalyst in Solvent-Free Synthesis of Polyhydroquinoline Derivatives: Green and Sustainable Protocol" 34 (12) (December 2020) e6000.

[16] F. Buazar, Impact of Biocompatible Nanosilica on Green Stabilization of Subgrade Soil, Sci Rep 9 (2019) 15147, https://doi.org/10.1038/s41598-019-51663-2.

[17] K. Sheoran, H. Kaur, S.S. Siwal, A.K. Saini, D.V.N. Vo, V.K. Thakur, Recent advances of carbon-based nanomaterials (CBNMs) for wastewater treatment: Synthesis and application, Chemosphere 299 (2022) 134364, https://doi.org/10.1016/j.chemosphere.2022.134364.

[18] N.H. Rezazadeh, F. Buazar, S. Matroodi, Synergistic effects of combinatorial chitosan and polyphenol biomolecules on enhanced antibacterial activity of biofunctionalized silver nanoparticles, Sci Rep 10 (2020) 19615, https://doi.org/10.1038/s41598-020-76726-7.

[19] B.S. Gholizadeh, F. Buazar, S.M. Hosseini, S.M. Mousavi, Enhanced antibacterial activity, mechanical and physical properties of alginate/hydroxyapatite bio nanocomposite film, Int. J. Biol. Macromol. 116 (2018) 786–792, https://doi.org/10.1016/j.ijbiomac.2018.05.104.

[20] N. Asghar, A. Hussain, D.A. Nguyen, S. Ali, I. Hussain, A. Junejo, Ali A (2024) Advancement in nanomaterials for environmental pollutants remediation: a systematic review on bibliometrics analysis, material types, synthesis pathways, and related mechanisms, J Nanobiotechnol 22 (2024) 26, https://doi.org/10.1186/s12951-023-02151-3.

[21] J. Lyu, L. Zhu, C. Burda, Considerations to improve adsorption and photocatalysis of low concentration air pollutants on TiO_2, Catal Today 225 (2014) 24–33, https://doi.org/10.1016/j.cattod.2013.10.089.

[22] P. Cervantes-Avilés, A.A. Keller, Incidence of metal-based nanoparticles in the conventional wastewater treatment process, Water Res. 189 (2021) 116603, https://doi.org/10.1016/j.watres.2020.116603.

[23] S. Ghotekar, T. Pagar, S. Pansambal, R. Oza, A review on green synthesis of sulfur nanoparticles via plant extract, characterization and its applications, Adv J Chem-Sect B Nat Prod Med Chem 2 (3) (2020) 128–143, https://doi.org/10.22034/ajcb.2020.109501.

[24] J. Yang, J. Du, X. Li, Y. Liu, C. Jiang, W. Qi, K. Zhang, C. Gong, R. Li, M. Luo, H. Peng, Highly hydrophilic TiO_2 nanotubes network by alkaline hydrothermal method for photocatalysis degradation of methyl orange, Nanomaterials 9 (4) (2019) 526, https://doi.org/10.3390/nano9040526.

[25] H. Sauf, M. El Alouani, S. Alehyen, M. El Achouri, J. Aride, Photocatalytic degradation of methylene blue from aqueous medium onto perlite-based geopolymer, Int J Chem Eng 2020 (2020) 9498349, https://doi.org/10.1155/2020/9498349.

[26] L.M. Anaya-Esparza, E. Montalvo-González, N. González-Silva, M.D. Méndez-Robles, R. Romero-Toledo, E.M. Yahia, A. Pérez-Larios, Synthesis and characterization of TiO_2-ZnO-MgO mixed oxide and their antibacterial activity, Materials 12 (5) (2019) 698, https://doi.org/10.3390/ma12050698.

[27] R. Dhanalakshmi, A. Pandikumar, K. Sujatha, P. Gunasekaran, Photocatalytic and antimicrobial activities of functionalized sol-gel embedded ZnO-TiO_2 nanocomposite materials, Mater. Express 3 (4) (2013) 291–300, https://doi.org/10.1166/mex.2013.1133.

[28] B. Ruj, B. Bishayee, R.P. Chatterjee, A. Mukherjee, A. Saha, J. Nayak, S. Chakrabortty, An economic strategy towards the managing of selenium pollution from contaminated water: A current state-of-the-art review, J. Environ. Manage. 304 (2022) 114143, https://doi.org/10.1016/j.jenvman.2021.114143.

[29] S. Singh, G.K. Sidhu, H. Singh, Removal of methylene blue dye using activated carbon prepared from biowaste precursor, Indian Chem Eng 61 (1) (2019) 28–39, https://doi.org/10.1080/00194506.2017.1408431.

[30] S. Naraginti, Y. Li, Preliminary investigation of catalytic, antioxidant, anticancer and bactericidal activity of green synthesized silver and gold nanoparticles using *Actinidia deliciosa*, J Photochem Photobiol B 170 (2017) 225–234.

[31] L. Gao, C. Yin, Y. Luo, G. Duan, Facile synthesis of the composites of polyaniline and TiO_2 nanoparticles using self-assembly method and their application in gas sensing, Nanomaterials 9 (4) (2019) 493, https://doi.org/10.3390/nano9040493.

[32] A.H. Mamaghani, F. Haghighat, C.-S. Lee, Gas phase adsorption of volatile organic compounds onto titanium dioxide photocatalysts, Chem Eng J 337 (2018) 60–73, https://doi.org/10.1016/j.cej.2017.12.082.
[33] F. Buazar, A. Cheshmehkani, M.Z. Kassaee, Nanosteel synthesis via arc discharge: media and current effects, J Iran Chem Soc 9 (2012) 151–156, https://doi.org/10.1007/s13738-011-0038-3.
[34] M.Z. Kassaee, F. Buazar, E. Motamedi, Effects of current on arc fabrication of Cu nanoparticles, J. Nanomater. 2010 (2010) 403197, https://doi.org/10.1155/2010/403197.